

Wavenumber Measurements of CO₂ Transitions in 1.5- μ m Atmospheric Window Using an External-Cavity Diode Laser

Che-Chung Chou,* Tyson Lin,† and Jow-Tsong Shy‡

*Department of Electrical Engineering, Dai-Yeh University, Chang-Hwa 51501, Taiwan, Republic of China; †Physics Teaching and Research Center, Feng Chia University, Taichung 40724, Taiwan, Republic of China; and ‡Department of Physics, National Tsing Hua University, Hsinchu 30013, Taiwan, Republic of China

Received July 24, 2000; in revised from September 19, 2000

Using an external-cavity diode laser (ECDL) as the light source, we have observed the spectrum of CO₂ in the 1.5- μ m atmospheric window including the (30⁰1)₁ ← (00⁰0) and (31¹1)₁ ← (01¹0)₁ bands. Good signal-to-noise ratio allowed us to lock the frequency of our ECDL to the absorption line centers. Wavenumber measurements of the transitions with accuracy about $6.6 \times 10^{-4} \text{ cm}^{-1}$ are made with the help of a precision wavemeter calibrated to the accurate C₂H₂ frequency references in the 1.5- μ m wavelength region. Molecular constants are obtained by making the least-squares fits of the measured transition wavenumbers. The rotational and centrifugal distortion constants are consistent with the previous results using high-resolution Fourier transform spectroscopy. However, the band centers are different with previous results by several thousandth reciprocal centimeters. © 2001 Academic Press

Key Words: external-cavity diode laser; CO₂; wavenumber measurements; C₂H₂; molecular constants.

1. INTRODUCTION

Due to the strong infrared activity of CO₂, the infrared spectrum of CO₂ plays an important role in many spectroscopic fields. For example, (i) it can be used as the wavenumber standards in the mid-infrared (1); (ii) CO₂ is the primary atmospheric absorber, hence its spectrum is a prime factor in atmospheric remote sensing; (iii) CO₂ is also the major source of near-infrared atmospheric opacity on Venus; therefore the emission spectrum of Venus are originated from the weak CO₂ bands at the hot surface (2). Most of the laboratory works on the CO₂ spectrum were made using the Fourier transform spectrometer (FTS), which might have resolution from several hundredth to several thousandth reciprocal centimeters. However, due to the white light source in FTS, weak transitions are difficult to detect. In general, weak CO₂ transitions are measured with very long path absorption cell or from the spectrum of the planets.

On the other hand, external-cavity diode lasers (ECDL) are being used increasingly in the spectroscopy of atoms or molecules because their intensity noises are very small and they provide enough power with narrow linewidth and widely tunable range of wavelength (3). ECDL is especially useful to accurately detect weak spectrum while the FTS is difficult to do. Significant developments of ECDL in the 1.5- μ m wavelength region have been made to fulfill the increasing demand for the fiber optic communication. Up to now, there are many commercial ECDL systems ready to be used in spectroscopy.

Besides, it is important in spectroscopy to accurately determine the wavenumber of the transitions. To reach this goal, many wavenumber standards for the infrared are recommended by the International Union of Pure and Applied Chemistry (1).

In Ref. (1), Doppler-limited spectrum of C₂H₂ with an accuracy of 10^{-7} (4) was chosen as the wavenumber standards in the 1.5- μ m wavelength region. Recently, using the technique of cavity-enhanced spectroscopy, de Labacherie *et al.* first successfully observed the saturated absorption of C₂H₂ lines (5), and then Nakagawa *et al.* measured the frequencies of 90 rovibrational lines of ¹²C₂H₂ and ¹³C₂H₂ with an accuracy of 10^{-9} (6). The results form an accurate frequency grid in the 1.5- μ m wavelength region for the spectroscopy as well as many other applications such as fiber communications.

In this paper, we report our study on the weak transitions of CO₂ in the 1.5- μ m wavelength region. To probe such a weak absorption, a commercial ECDL was used as the light source and a multipass cell was used to increase the absorption length. With them, the spectrum of CO₂ (30⁰1)₁ ← (00⁰0) and (31¹1)₁ ← (01¹0)₁ bands were clearly observed. The wavenum-

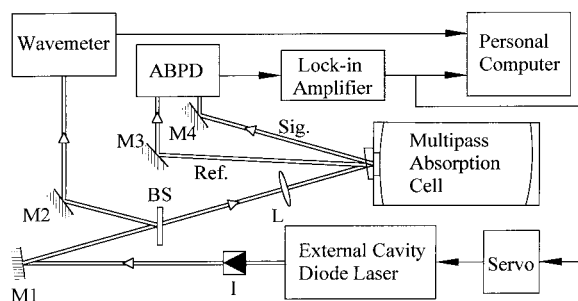


FIG. 1. Experimental setup. I: optical isolator; BS: beam splitter; M1–M4: mirrors; L: lens; Ref.: reference laser beam; Sig.: signal laser beam; ABPD: auto-balanced photodetector. The reference laser beam is the beam reflected on the tilted entrance window of the multipass absorption cell, while the signal laser beam is the output of the multipass absorption cell.

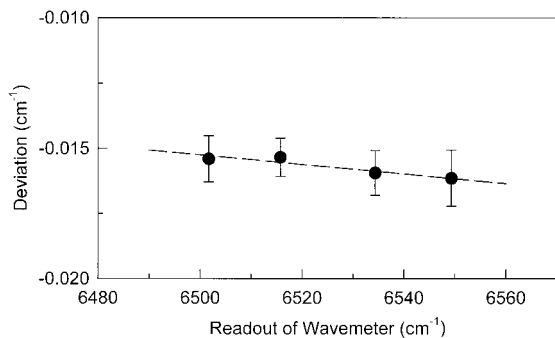


FIG. 2. A plot of the deviations between the measured results of chosen ¹²C₂H₂ lines and the values of Ref. (6) vs. the readouts of wavemeter. The error bars shown are 1σ standard deviation of the measurements.

ber of the observed transitions were also measured. To ensure the accuracy of our measurements, accurate values of ¹²C₂H₂ transition wavenumbers by Nakagawa *et al.* (6) were used as the frequency references to calibrate our wavemeter.

2. EXPERIMENTAL DETAILS

A schematic diagram of our experiment setup is shown in Fig. 1. To probe the weak transitions, we used an ECDL (Environmental Optical Sensor, Inc., model 2001) as the powerful but “clean” light source in our experiment. The linewidth of the ECDL is less than 1 MHz and the single-mode frequency tuning range is 60 GHz. The laser frequency was frequency-modulated at 1 kHz with a modulation depth of 21 MHz. The modulated laser beam was then split by a beam splitter (BS), which reflects 10% of incident power to the wavemeter (Burleigh, model WA-1500 NIR, 0.1 ppm accuracy) for wavenumber measurement, and transmitted 90% of incident power to the

multipass cell (New Focus, model 5612) for the absorption spectroscopy. The multipass cell has a path length of 100 m. Pure CO₂ gas (99.9%) of pressure 16 to 20 Torr was filled into this cell. At this low pressure, the pressure shift is much smaller than the uncertainty of our wavenumber measurement and can be neglected. Since the entrance window of the multipass cell is tilted, the laser beam reflected by this window was sent to the reference port of the auto-balanced photodetector (New Focus, model 2017). This beam served as a reference laser beam to balance the variation of laser power. The signal laser beam after passing through the multipass cell was sent to the signal port of the auto-balanced photodetector. The auto-balanced output from the photodetector was demodulated by the lock-in amplifier (Stanford Research, model SR830) and was recorded by a personal computer through the GPIB interface and LabVIEW program.

To determine the center of a transition line, we first tuned ECDL over the full width of a transition line and recorded its first derivative signal. If the signal-to-noise ratio was good enough, then ECDL was tuned back to the center of the transition line, and then the servo loop was turned on to lock the frequency of ECDL to this line center. Then the wavelength of ECDL measured by the wavemeter was recorded for 1 min.

3. CALIBRATION

To ensure the measurements having the nominal accuracy of our wavemeter, the readouts of wavemeter was carefully calibrated to the transition frequencies of ¹²C₂H₂ given by Nakagawa *et al.* (6). Here we chose the *P*(3), *P*(9), *P*(16), and *P*(21) lines of ¹²C₂H₂ ν₁ + ν₃ band as our references. For this purpose, instead of the multipass cell in Fig. 1, the signal laser beam passed through a cell 20 cm long filled with ¹²C₂H₂ gas of pressure less than 1 Torr. The pressure

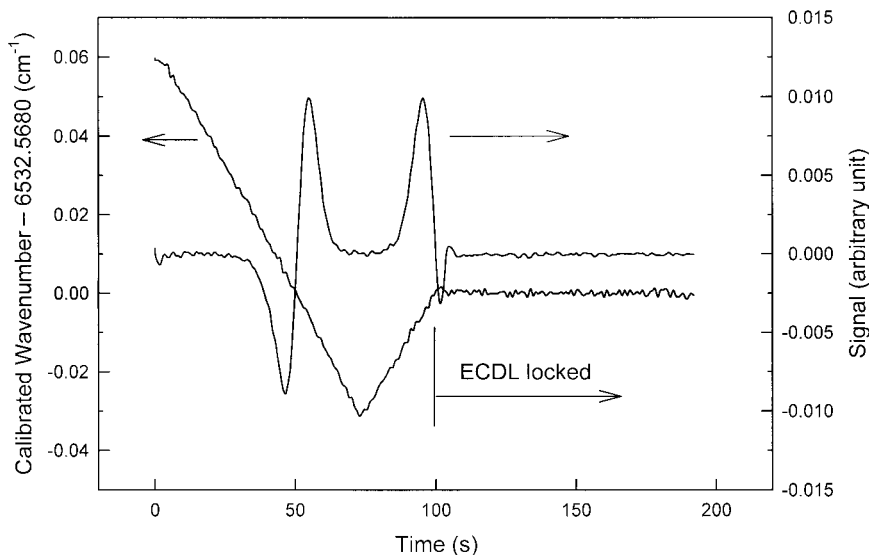


FIG. 3. Result of the wavenumber measurement of CO₂ (30⁰1)₁ ← (00⁰0) band *R*(42) line.

TABLE 1
Results (in cm^{-1}) of Wavenumber Measurement of CO_2 (30^0_1) \leftarrow (00^0_0) Band

R-Branch				P-Branch			
J	Obs. Freq.	Std. Dev. ^a	Obs. - Calc.	J	Obs. Freq.	Std. Dev. ^a	Obs. - Calc.
0	6503.8553	0.0010	0.0002				
2	6505.3937	0.0008	0.0002	2	6501.5137	0.0008	0.0000
4	6506.9143	0.0009	0.0003	4	6499.9301	0.0009	-0.0004
6	6508.4173	0.0010	0.0007	6	6498.3287	0.0010	-0.0006
8	6509.9012	0.0008	-0.0000	8	6496.7103	0.0008	-0.0001
10	6511.3685	0.0008	0.0003	10	6495.0728	0.0009	-0.0011
12	6512.8177	0.0025	0.0003	12	6493.4200	0.0008	0.0002
14	6514.2490	0.0008	0.0001	14	6491.7481	0.0007	-0.0000
16	6515.6635	0.0009	0.0004	16	6490.0592	0.0008	-0.0002
18	6517.0602	0.0007	0.0002	18	6488.3533	0.0009	-0.0002
20	6518.4398	0.0006	0.0000	20	6486.6308	0.0008	-0.0000
22	6519.8027	0.0005	0.0001	22	6484.8913	0.0007	-0.0003
24	6521.1499	0.0009	0.0010	24	6483.1356	0.0008	-0.0003
26	6522.4789	0.0007	0.0001	26	6481.3639	0.0008	-0.0004
28	6523.7926	0.0005	0.0001	28	6479.5767	0.0006	-0.0002
30	6525.0905	0.0007	-0.0000	30	6477.7741	0.0009	-0.0000
32	6526.3733	0.0006	0.0003	32	6475.9560	0.0008	-0.0003
34	6527.6406	0.0005	0.0001	34	6474.1239	0.0008	0.0001
36	6528.8935	0.0006	0.0002	36	6472.2764	0.0008	-0.0007
38	6530.1318	0.0007	0.0001	38	6470.4164	0.0007	-0.0002
40	6531.3567	0.0005	0.0003	40	6468.5426	0.0007	-0.0002
42	6532.5680	0.0006	0.0003	42	6466.6560	0.0006	-0.0004
44	6533.7664	0.0010	0.0001	44	6464.7570	0.0010	-0.0004
46	6534.9530	0.0006	0.0005	46	6462.8468	0.0007	-0.0001
48	6536.1271	0.0006	0.0001	48	6460.9246	0.0009	-0.0006
50				50	6458.9919	0.0006	-0.0011
52	6538.4439	0.0005	0.0007	52	6457.0503	0.0006	-0.0006
54	6539.5869	0.0009	0.0005	54	6455.0999	0.0009	0.0001
56	6540.7199	0.0010	-0.0005	56	6453.1403	0.0008	0.0002
58	6541.8459	0.0005	-0.0001	58			

^a These are the standard deviations of the wavenumber readouts measured after the laser frequency locked to the line center.

shift of $^{12}\text{C}_2\text{H}_2$ gas is less than 200 kHz/Torr (7). With pressure less than 1 Torr, we can assure that the pressure shift of $^{12}\text{C}_2\text{H}_2$ gas is well within the uncertainty of our wavenumber measurement. We first locked our ECDL to the center of the Doppler profile of each chosen $^{12}\text{C}_2\text{H}_2$ line and then measured the wavenumber using our wavemeter. Figure 2 is a plot of the deviations between the measured results and the values of Ref. (6) vs. the readouts of wavemeter. The solid points, in the order of increasing wavenumber, correspond to the deviations of the $P(21)$, $P(16)$, $P(9)$, and $P(3)$ lines of $^{12}\text{C}_2\text{H}_2$ $\nu_1 + \nu_3$ band, respectively. This plot shows that the deviations are linearly dependent on our wavemeter readouts. Hence we fit the deviations to a linear function of the wavemeter readouts. The dashed line in Fig. 2 is the fitted result. The resulting function is then used as our calibrating function to obtain the calibrated values. The differences of the calibrated values and the values given by Ref. (6) are no more than $1.7 \times 10^{-4} \text{ cm}^{-1}$. After this calibration procedure, the wavemeter can be used with its nominal accuracy, which is about $6.5 \times 10^{-4} \text{ cm}^{-1}$, in this work.

4. RESULTS

A typical result of wavenumber measurement is shown in Fig. 3. In this figure, the measurement of $R(42)$ transition of CO_2 (30^0_1) \leftarrow (00^0_0) band is given as an example. At least 1 min long of wavenumber readouts were recorded after the ECDL was frequency locked. These readouts were then averaged and yielded the line center for the corresponding transition. The standard deviation of the above readouts was also calculated, and its reciprocal of squares will be used as the weightings in the least-squares analysis.

In Fig. 3, the frequency difference between the peak-to-peak of the first derivative signal is small and estimated to be 0.011 cm^{-1} (its full width of half-maximum is about 0.019 cm^{-1}). Therefore, the first derivative signal is more sensitive to the frequency variation than the readouts of our wavemeter. We can see from Fig. 3 that the variation of the residual error signal is smaller than the variation of wavemeter readouts. Hence we expect that the actual stability of the laser locked to a CO_2 transition is much better than the standard deviation calculated from the wavemeter readouts. The statistical error of each line

TABLE 2
Results (in cm⁻¹) of Wavenumber Measurement of CO₂ (31¹e)₁ ← (01¹0e)₁ Band

R-Branch				P-Branch			
J	Obs. Freq.	Std. Dev. ^a	Obs. - Calc.	J	Obs. Freq.	Std. Dev. ^a	Obs. -Calc.
1				1			
3	6539.5097	0.0006	0.0005	3	6534.0833	0.0006	0.0004
5	6541.0053	0.0010	0.0006	5	6532.4780	0.0005	0.0002
7	6542.4767	0.0005	0.0008	7	6530.8492	0.0010	0.0008
9	6543.9234	0.0006	0.0006	9	6529.1944	0.0006	-0.0005
11	6545.3456	0.0010	0.0003	11	6527.5166	0.0005	-0.0005
13	6546.7437	0.0006	0.0001	13	6525.8153	0.0005	-0.0002
15	6548.1181	0.0005	0.0003	15	6524.0892	0.0006	-0.0007
17	6549.4685	0.0007	0.0007	17	6522.3397	0.0005	-0.0008
19	6550.7945	0.0008	0.0006	19	6520.5667	0.0005	-0.0007
21	6552.0965	0.0006	0.0004	21	6518.7702	0.0005	-0.0006
23	6553.3744	0.0005	-0.0001	23			
25				25	6515.1075	0.0009	-0.0004
27				27	6513.2415	0.0007	-0.0003
29	6557.0693	0.0006	0.0006	29			
31	6558.2540	0.0006	0.0004	31	6509.4412	0.0008	-0.0003
33	6559.4165	0.0007	0.0010	33	6507.5074	0.0011	-0.0003
35	6560.5551	0.0005	0.0003	35	6505.5517	0.0008	-0.0002
37	6561.6716	0.0009	0.0000	37	6503.5735	0.0008	-0.0007
39				39	6501.5754	0.0008	0.0005
41				41	6499.5545	0.0009	0.0001
43				43	6497.5120	0.0007	-0.0010

^a These are the standard deviations of the long wavenumber readouts measured after the laser frequency locked to the line center.

center measurement is too small to be taken into account in the experimental errors. However, the offset from line center of each frequency-lock may contribute to the inaccuracy of each line center measurement. Estimated from the residual error signal, the typical offsets of our frequency-lock are 1.0×10^{-4} cm⁻¹. Hence, combining with the 6.5×10^{-4} cm⁻¹ accuracy of wavemeter independently, the accuracy of each line center measurement is about 6.6×10^{-4} cm⁻¹.

The measured wavenumbers of the (30⁰1)₁ ← (00⁰0) band and the two (31¹1)₁ ← (01¹0) subbands are summarized in Tables 1, 2, and 3, respectively. In addition to lines of high- or low-rotational quantum number which are too weak to be measured, there are still several lines missing in the tables. This is because they accidentally overlap with other stronger lines, and significant frequency pullings of these weak lines were observed. Therefore we did not include these pieces of data in the tables.

5. ANALYSES AND DISCUSSION

(i) (30⁰1)₁ ← (00⁰0) Band

The molecular constants of this band were first given by Mandin (8) based on the Venus infrared spectrum (9). Later, Maillard *et al.* made an observation of this band in the laboratory using a very high-resolution FTS (10). A set of more accurate constants were also given in their paper. Since both works used the FTS, it is worth comparing our work, which is

based on the laser spectroscopy and a more accurate frequency standard, with the previous works.

The ground state (00⁰0) had been measured in a lot of observations of different bands. Molecular constants of the ground state based on these measurements were given in the paper of Rothman *et al.* (11), which used the global fits to obtain more accurate constants. To this point, we fixed the molecular constants (*B''*, *D''*, *H''*) of the ground state to the values given by Ref. (11) in our least-squares fit. We fitted the molecular constants (*B'*, *D'*, *H'*) of (30⁰1)₁ state, and the band center ν_0 , using the formula

$$\begin{aligned} \nu = & \nu_0 + B'm(m+1) - D'm^2(m+1)^2 + H'm^3 \\ & \times (m+1)^3 - B''m(m-1) + D''m^2(m-1)^2 [1] \\ & - H''m^3(m-1)^3, \end{aligned}$$

where $m = -J$ for the *P* branch and $m = J + 1$ for the *R* branch. The results are summarized in Table 4. The molecular constants were then used to calculate the transition frequencies of the (30⁰1)₁ ← (00⁰0) band. The differences between the observed frequencies and the calculated frequencies are listed in the fourth column of Table 1. The variance of this fit is 3.9×10^{-4} cm⁻¹.

Also listed in Table 4 are the constants given by Refs. (10) and (11) for comparison. Our results of rotational and centrifugal distortion constants are close to those of Refs. (10) and

TABLE 3
Results (in cm^{-1}) of Wavenumber Measurement of CO_2 ($31^11f_1 \leftarrow (01^10f_1$ Band

R-Branch				P-Branch			
J	Obs. Freq.	Std. Dev. ^a	Obs. - Calc.	J	Obs. Freq.	Std. Dev. ^a	Obs. - Calc.
0				0			
2				2			
4	6540.2952	0.0009	0.0006	4	6533.2899	0.0010	0.0001
6	6541.8053	0.0010	0.0004	6	6531.6876	0.0005	0.0005
8	6543.2993	0.0005	0.0007	8	6530.0675	0.0016	-0.0003
10	6544.7750	0.0007	-0.0005	10	6528.4312	0.0006	-0.0007
12	6546.2357	0.0006	-0.0001	12	6526.7790	0.0005	-0.0005
14	6547.6799	0.0007	0.0005	14			
16	6549.1066	0.0007	-0.0000	16	6523.4245	0.0006	-0.0012
18	6550.5175	0.0007	0.0002	18	6521.7246	0.0009	-0.0000
20	6551.9122	0.0005	0.0004	20	6520.0063	0.0006	-0.0012
22	6553.2900	0.0005	-0.0000	22	6518.2747	0.0009	0.0000
24				24	6516.5262	0.0007	-0.0001
26	6555.9999	0.0006	0.0012	26	6514.7620	0.0007	-0.0004
28	6557.3296	0.0006	0.0001	28	6512.9829	0.0012	-0.0005
30	6558.6461	0.0008	0.0013	30	6511.1894	0.0009	-0.0001
32	6559.9455	0.0006	0.0007	32	6509.3792	0.0008	-0.0016
34	6561.2298	0.0008	-0.0001	34	6507.5574	0.0009	-0.0003
36				36	6505.7202	0.0010	-0.0003
38				38			
40				40	6502.0047	0.0009	0.0001
42				42			
44				44	6498.2356	0.0009	-0.0004

^a These are the standard deviations of the wavenumber readouts measured after the laser frequency locked to the line center.

(11), but the band centers are significantly different from each other. Although the data of Ref. (10) is included in the data bank for the global fits, the band center of Ref. (11) is much closer to our result. The reason is not clear and is to be further investigated. One possible cause is, since absolute wavenumbers rather than relative wavenumbers are required to accurately determine the band center, the deviations are probably due to the different frequency references used in our work and Maillard *et al.* (10).

(ii) (31^11)₁ \leftarrow (01^10)₁ Band

In this band, the splitting of *e* and *f* levels is due to the rovibrational interaction affecting only one of the two degenerate ν_2 mode. Therefore, in our fittings, the *e* and *f* levels were treated as separate states with different values of the rotational and centrifugal distortion constants which are relative to the rotation of the molecule. But the band centers, which are independent of the rotation of the molecule, were forced to be the same.

This band had been observed in the Venus infrared spectrum (9) and was identified by Mandin (8). In the case of the lower state (01^10)₁, a lot of measurements from observations of different bands have been made. Global-fitted molecular constants of lower state based on these measurements are also given in Ref. (11). Again, we fixed the molecular constants (B''_e , D''_e , H''_e , B''_f , D''_f , H''_f) of the lower state to the values

given by Ref. (11) in our least-squares fit. We fitted the molecular constants (B'_e , D'_e , B'_f , D'_f) of (31^11)₁ state and the band center ν_0 , using the formulas

$$\begin{aligned} \nu = \nu_0 + F_+(m)[B'_e m(m+1) - D'_e m^2(m+1)^2 - B''_e m \\ \times (m-1) + D''_e m^2(m-1)^2 - H''_e m^3(m-1)^3] \\ + F_-(m)[B'_f m(m+1) - D'_f m^2(m+1)^2 \\ - B''_f m(m-1) + D''_f m^2(m-1)^2 - H''_f m^3(m-1)^3], \end{aligned} \quad [2]$$

TABLE 4
Molecular Constants (in cm^{-1}) of CO_2 (30^01)₁ \leftarrow (00^00) Band

constant	this work ^a	Ref. 11	Ref. 10 ^c
ν_0	6503.07906(13)	6503.0809	6503.083981(37)
$B_{(30^01)_1}$	0.38797607(39)	0.38797369	0.38797686(2)
$D_{(30^01)_1} \times 10^7$	0.7450(28)	0.71684	0.7499(15)
$H_{(30^01)_1} \times 10^{13}$	7.49(54)		7.62(39)
$B_{(00^00)}$	0.39021889 ^b	0.39021889	0.39021932(47)
$D_{(00^00)} \times 10^7$	1.33338 ^b	1.33338	1.3356(12)
$H_{(00^00)} \times 10^{13}$	0.077 ^b	0.077	

^a The numbers in parentheses are the standard errors in unit of last significant digit.

^b Constants are fixed to Ref. (11).

TABLE 5
Molecular Constants (in cm⁻¹) of CO₂ (31¹)₁ ← (01¹0)₁ Band

constant	this work ^a	Ref. 11	Ref. 8 ^a
ν_0	6536.44498(14)	6536.4490	6536.4496(3) ^c 6536.4497(4) ^d
$B_{(31^1 1e)_1}$	0.38759448(62)	0.38759651	0.38759651(120)
$D_{(31^1 1e)_1} \times 10^7$	0.9900(41)	0.99	0.9947(12)
$B_{(31^1 1f)_1}$	0.38915604(59)	0.38915188	0.38915188(847)
$D_{(31^1 1f)_1} \times 10^7$	0.9536(42)	0.94	0.9357(30)
$B_{(01^1 0e)_1}$	0.39063900 ^b	0.39063900	0.3906402(24)
$D_{(01^1 0e)_1} \times 10^7$	1.35295 ^b	1.35295	1.3599(5)
$H_{(01^1 0e)_1} \times 10^{13}$	0.099 ^b	0.099	
$B_{(01^1 0f)_1}$	0.39125465 ^b	0.39125465	0.3912533(39)
$D_{(01^1 0f)_1} \times 10^7$	1.36088 ^b	1.36088	1.3576(8)
$H_{(01^1 0f)_1} \times 10^{13}$	0.1490 ^b	0.149	

^a The numbers in parentheses are the standard errors in unit of last significant digit.

^b Constants are fixed to Ref. (11).

^c Band center of (31¹1e)₁ ← (01¹0e)₁ subband.

^d Band center of (31¹1f)₁ ← (01¹0f)₁ subband.

and

$$F_{\pm}(m) = \frac{1}{2} \left[1 \pm \frac{m(-1)^m}{|m|} \right], \quad [3]$$

where $m = -J$ for the P branch and $m = J + 1$ for the R branch. The function F is used to determine whether the m value is corresponding to an e level (F_+) or an f level (F_-). The molecular constants were then used to calculate the transition frequencies of the (31¹1)₁ ← (01¹0)₁ band. The differences between the observed frequencies and the calculated frequencies of the (31¹1e)₁ ← (01¹0e)₁ and (31¹1f)₁ ← (01¹0f)₁ subbands are listed in the fourth column of Tables 2 and 3, respectively. The variance of this fit is $6.1 \times 10^{-4} \text{ cm}^{-1}$.

The results are summarized in Table 5 along with the values given by Refs. (8) and (11) for comparison. In this case, the rotational and the centrifugal distortion constants and the band centers of our works show significant deviations from Refs. (8) and (11). The work of Ref. (8) was based on the Venus infrared spectrum (9), which is far less accurate than laser spectroscopy of this work. In fact, the results of Ref. (8) were the only source for this band in the global fit of Ref. (11). Hence the band center and the upper state constants of Ref. (11) are very close to the results of Ref. (8).

6. CONCLUSIONS

The weak CO₂ transitions of the (30⁰1)₁ ← (00⁰0) and (31¹1)₁ ← (01¹0)₁ bands in the 1.5-μm atmospheric window have been studied by laser spectroscopy using an external-

cavity diode laser and the C₂H₂ frequency standards. New molecular constants are obtained by the least-squares fits of the measured transition wavenumbers and are compared with the previous works. Our constants are close to those using high-resolution FTS and show significant deviation from those obtained from planet spectrum. However, our band centers are significantly different from previous works. The reason is probably due to the different frequency references used in our work and the previous works. Currently we are preparing to make heterodyne frequency measurements of the CO₂ transitions against the C₂H₂ frequency standards. This will help us to confirm the accuracy of the measurements made with our wavemeter.

The spectrum obtained by this experiment shows that this method can also be used to study other Doppler-limited weak transitions in this wavelength region. However, to further probe much weaker transitions beyond this work and to make a sub-Doppler-limited spectroscopy, one should consider a laser spectroscopy method of higher sensitivity, such as the “noise-immune cavity-enhanced optical heterodyne molecular spectroscopy” (NICE-OHMS) demonstrated by Ye *et al.* (12).

ACKNOWLEDGMENTS

The authors express thanks to Prof. C.-C. Tsai for lending them his new wavemeter which played an important role in this work. This work was supported by the National Science Council of R.O.C. under the Contract Nos. NSC-87-2112-M-212-002 and NSC-88-2112-M-212-001.

REFERENCES

1. G. Guelachvil, M. Birk, Ch. J. Borde, J. W. Brault, L. R. Brown, B. Carli, A. R. H. Cole, K. M. Evenson, A. Fayt, D. Hausamann, J. W. C. Johns, J. Kauppinen, Q. Kou, A. G. Maki, K. Naraharirao, R. A. Toth, W. Ubran, A. Valentin, J. Verges, G. Wagner, M. H. Wappelhorst, J. S. Wells, B. P. Winnewisser, and M. Winnewisser, *J. Mol. Spectrosc.* **177**, 164–179 (1996).
2. R. W. Carlson, K. H. Baines, Th. Encrenaz, F. W. Taylor, P. Drossart, L. W. Kamp, J. B. Pollack, E. Lellouch, A. D. Collard, S. B. Calcutt, D. Grinspoon, P. R. Weissman, W. D. Smythe, A. C. Ocampo, G. E. Danielson, F. P. Fanale, T. V. Johnson, H. H. Kieffer, D. L. Matson, T. McCord, and L. A. Soderblom, *Science* **253**, 1541–1548 (1991).
3. C. E. Wieman and L. Hollberg, *Rev. Sci. Instrum.* **62**, 1–20 (1991).
4. H. Sasada, S. Takeuchi, M. Iritani, and K. Nakatani, *J. Opt. Soc. Am. B: Opt. Phys.* **8**, 713–718 (1991).
5. M. de Labachellerie, K. Nakagawa, and M. Ohtsu, *Opt. Lett.* **19**, 840–842 (1994).
6. K. Nakagawa, M. de Labachellerie, Y. Awaji, and M. Kourogi, *J. Opt. Soc. Am. B: Opt. Phys.* **13**, 2708–2714 (1996).
7. Y. Sakai, S. Sudo, and T. Ikegami, *IEEE J. Quantum Electron.* **28**, 75–81 (1992).
8. J.-Y. Mandin, *J. Mol. Spectrosc.* **67**, 304–321 (1977).
9. P. Connes and G. Michel, *Astrophys. J.* **190**, L29–L32 (1974).
10. J. P. Maillard, M. Cuisenier, Ph. Arcas, E. Arie, and C. Amiot, *Can. J. Phys.* **58**, 1560–1569 (1980).
11. L. S. Rothman, R. L. Hawkins, R. B. Wattson, and R. R. Gamache, *J. Quant. Spectrosc. Radiat. Transfer* **48**, 537–566 (1992).
12. J. Ye, L.-S. Ma, and J. L. Hall, *J. Opt. Soc. Am. B: Opt. Phys.* **15**, 6–15 (1998).